Comparative Medicine
Copyright 2017
by the American Association for Laboratory Animal Science

Vol 67, No 4
August 2017
Pages 350–355

Original Research

Differences in Vascular Response between Balloon Overstretch and Stent Overexpansion in Nonatherosclerotic Porcine Coronary Arteries

Yoshiaki Mitsutake,[1,†] Jörg Reifart, [1,†] Wook Bum Pyun,[2,†] Jennifer K Lyons,[1] Tobias Deuse,[3] Sonja Schrepfer,[3] and Fumiaki Ikeno[1,*]

Which preclinical models are best suited for restenosis research remains uncertain. Here we compared the restenotic responses after balloon or stent overstretch injury in a porcine coronary artery. A total of 30 coronary lesions in 5 pigs were treated by balloon overdilatation or oversized stent implantation at various balloon-to-artery (B:A) ratios. Four weeks later, the lesions were examined in vivo by using coronary angiography, intravascular ultrasound, and optical coherence tomography (OCT). At follow-up, the lumen area stenosis and plaque burden at the minimal lumen area site were greater in stented sites than in balloon injury site (lumen area stenosis, 21.7 ± 8.9% compared with 32.8 ± 12.1%; plaque burden, 30.1% ± 10.1% compared with 44.7% ± 10.1%, respectively). The remodeling index was significantly smaller for the balloon-injury group than the stent group (0.86 ± 0.11 compared with 1.00 ± 0.04). Only the stent group that was dilated at a high B:A ratio resulted in increased plaque burden. In the balloon-injury sites, high B:A ratios were significantly associated with greater negative remodeling. Tissue morphology assessment by OCT revealed that the predominant pattern in balloon injury sites was homogeneous, whereas that in stented sites was a layered to heterogeneous pattern. Neointimal proliferation was significantly greater after oversized stenting than after balloon overstretch injury. Together these findings suggest that stent overexpansion of porcine coronary arteries might be appropriate for researching restenosis than is the balloon overstretch injury model.

Abbreviations: BMS, bare-metal stents; CSA, cross-sectional area; DES, drug-eluting stents; EEM, external elastic membrane; IVUS, intravascular ultrasonography; MLA, minimal lumen area; OCT, optical coherence tomography; QCA, quantitative coronary angiography

Coronary intervention has evolved from balloon angioplasty, atherectomy, and bare-metal stenting (BMS) to implanting drug-eluting stents (DES). Consequently, the restenosis rate has been reduced dramatically but not completely eliminated, even in the DES era. Therefore, experimental efforts to prevent restenosis by using various pharmacologic agents and mechanical devices are underway.[1,4]

Optimal preclinical models of restenosis are needed so that restenosis-preventing therapies and new medical devices can be tested appropriately. Various animal models have been used for restenosis research, ranging from rats and rabbits to sheep and swine. However, the porcine nonatherosclerotic coronary artery restenosis model is the most useful, practical, and adaptable model because of its similarity to humans in terms of size, anatomy, and response after vessel injury.[16,17,21,22] In addition, the same equipment and techniques as in human coronary angioplasty are used, which is a great advantage of this model.[5,6,19,20] When porcine coronary arteries are injured by overstretch balloon angioplasty, a typical medial laceration occurs and is filled by neointima identical to human restenotic neointima.[4,7] Pigs are not only used in balloon overstretch models but also coronary stent restenosis models. Stent overexpansion can induce severe arterial injury and considerable coronary artery restenosis.[7]

In experimental restenosis studies, large volumes of new neointimal hyperplasia are required to evaluate potential therapies for restenosis. However, few studies have compared neointimal growth after balloon injury with that after stent overexpansion.[7] In the current study, we used intravascular ultrasonography (IVUS) to assess the extent of neointimal hyperplasia and to examine the relationship between the magnitude of neointimal hyperplasia and the degree of vessel injury in the nonatherosclerotic porcine coronary models of balloon overstretch injury and stent overexpansion. In addition, we evaluated whether optical coherence tomography (OCT) revealed differences in neointimal tissue characteristics between balloon overstretch and stent overexpansion model.

Materials and Methods

Animals and procedures. Animal care and study procedures were done in accordance with a protocol by the Stanford University Administrative Panel on Laboratory Animal Care (no.

Received: 14 Dec 2016. Revision requested: 30 Jan 2017. Accepted: 17 Feb 2017.
[1]Division of Cardiovascular Medicine, Stanford University, Stanford, California; [2]Department of Internal Medicine, Ewha Woman's University School of Medicine, Seoul, Korea; and [3]Department of Cardiovascular Surgery, University Heart Center–Hamburg, Hamburg, Germany.
[*]Corresponding author. Email: fikeno@stanford.edu
[†]The first 3 authors contributed equally to this work.

APLAC-11639) and followed the guidelines in the AALAS Position Statement for Humane Care and Use of Laboratory Animals. A total of 5 SPF, female, juvenile Yorkshire Swine (*Sus scrofa*; weight, 30 to 45 kg) were obtained from a local commercial farm (Pork Power, Turlock, CA) and maintained on free-choice food (product no. 203S, Nature's Match Sow and Pig Complete Feed, Purina Mills, St Louis, IL) and tap water. The animals were allowed to acclimate for at least 48 h. All animals were housed in individual pens, under a 12:12-h light:dark cycle (lights on, 0700 to 1900), at a temperature of 68 to 76 °F (20.0 to 24.4 °C).

Aspirin (650 mg) and nifedipine (30 mg) were administered orally at least 12 h prior to the procedure, and aspirin (81 mg) was continued for the duration of the study. The swine were fasted overnight and then sedated by using an intramuscular injection of tiletamine–zolazepam (6 mg/kg), followed by inhalant mask induction (isoflurane, 4% to 5%). After intubation, anesthesia was maintained by using 1% to 3% isoflurane in oxygen. For analgesia, carprofen (2 mg/kg) and buprenorphine (0.005 to 0.01 mg/kg) were administered intramuscularly prior to the procedure. The pigs were instrumented with auricular catheters and identified with numbered ear tags. After the introduction of an arterial sheath in the right or left femoral artery, an 8-French guiding catheter was inserted into the ostium of the coronary artery. The animals received heparin intravenously (300 U/kg) to maintain an activated clotting time of greater than 300 s. Baseline coronary angiography was performed to identify an optimal injury site according to artery size. The sizes of angioplasty balloon and stent were chosen on the basis of the estimated vessel diameter at the target lesion. After advancing a 0.014-in. guidewire into the target vessel, a BMS was deployed to achieve a balloon-to-artery (B:A) ratio of greater than 1.1:1 in stent overexpansion model. Balloon overstretch injury was produced at least 10 mm proximal from the stented site to achieve a B:A ratio of greater than 1.3:1. The balloon was inflated for 30 s twice, with a 30-s interval. Three coronary arteries—the left anterior descending artery, circumflex artery, and right coronary artery—were treated in all animals. Subsequently, vessel patency was confirmed by coronary angiography. The swine were then allowed to recover, after which they were monitored and received 81 mg aspirin daily for the duration of the study.

The swine underwent follow-up coronary angiography at 4 wk. At the same time, IVUS and OCT examinations were performed for all treated vessels. At the end of the study, the animals were euthanized with an intravenous bolus of potassium chloride (74.5 mg/kg) while under deep inhalant anesthesia.

Quantitative coronary analysis. The obtained angiograms were evaluated and analyzed by using QAngio XA software (version 7.3, Medis, Leiden, Netherlands). At follow-up, the balloon injury sites were identified relative to their distance to the stented site. The quantitative coronary analysis (QCA) parameters of minimal lumen diameter, reference vessel diameter, and percentage diameter stenosis were measured. Late loss was defined as the difference between the minimal luminal diameter immediately after the procedure and at follow-up. The B:A ratio was calculated as the mean diameter of the fully dilated balloon:mean diameter of the native (undilated) vessel.

IVUS evaluation. All IVUS examinations were performed after intracoronary administration of 0.2 mg nitroglycerin. Imaging assessment by IVUS was conducted by using Atlantis SR Pro 40 MHz catheters (Boston Scientific, Natick, MA) with an automated pullback speed of 0.5 mm/s. The IVUS catheters were positioned at least 5 mm distal of the stented site and then pulled back at least 5 mm proximal to the edge of the balloon injury site. The images were recorded and later analyzed by using Echoplaque version 3.0.38 software (INDEC Medical Systems, Santa Clara, CA).

IVUS measurements included the cross-sectional areas (CSA) of the external elastic membrane (EEM), lumen, and plaque (plaque = EEM – lumen). The percentage of lumen area stenosis was calculated as mean lumen CSA – minimal lumen area [MLA]) / mean lumen CSA × 100%. The percentage obstruction of the stent area was also calculated as: (intrastent plaque area/stent area) × 100%. Plaque burden (plaque / EEM CSA × 100) was reported from the slice containing the MLA site. The remodeling index was calculated as the EEM CSA at the MLA site divided by the average of the proximal and distal reference segment EEM CSA.[11] When the lesion EEM area is greater than the reference EEM area, positive remodeling has occurred, and the index will be greater than 1.0. If the lesion EEM area is smaller than the reference EEM area, negative remodeling has occurred, and the index will be less than 1.0.

OCT assessment. All OCT examinations (M2 system, LightLab Imaging–St Jude Medical, Westford, MA) were performed after intracoronary injection of 0.2 mg nitroglycerin. During image acquisition, the occlusion balloon was inflated at 0.4 to 0.8 atm, and saline was infused at 0.6 to 1.0 mL/s. The image catheter was pulled from distal to proximal by using a motorized pullback system at 1.0 mm/s, and continuous images were stored digitally for subsequent analysis. Analysis of the OCT images at 1-mm longitudinal intervals was performed by using proprietary software (LightLab Imaging).

Neointimal tissue was evaluated qualitatively according to a published OCT classification system, which recognizes 3 patterns: homogeneous, layered, and heterogeneous.[2,13,23] The homogeneous pattern comprises a uniformly signal-rich structure. The layered pattern has a signal-poor appearance with a high-signal band adjacent to the luminal surface. The heterogeneous pattern was identified as the presence of several varied signals. When multiple patterns were seen, the dominant pattern was adopted. Representative cases of each type of tissue structure and backscatter are shown in Figure 1.

Statistical analysis. All continuous data are given as mean ± 1 SD. For intergroup comparisons, an unpaired *t* test was applied to continuous variables. To examine the correlations between the measured variables, a regression analysis was applied to each set of measured variables. Categorical variables are presented as percentages (%). The χ^2 test was used for categorical variables. A 2-tailed *P* value less than 0.05 was considered statistically significant. All statistical analyses were performed by using SPSS (version 22.0, SPSS, Chicago, IL).

Results

A total of 30 sites in 15 vessels were treated by using balloon injury or stent implantation. At follow-up, one angiogram was unavailable, and we were unable to obtain IVUS and OCT images of 2 stented sites due to the extent of neointimal hyperplasia, which prevented the imaging catheters from passing the lesions. Consequently, we analyzed 28 treated sites (balloon injury, 14; stent, 14) by QCA and 28 IVUS images (balloon injury, 15; stent, 13). For tissue characterization, we analyzed 388 cross-sectional

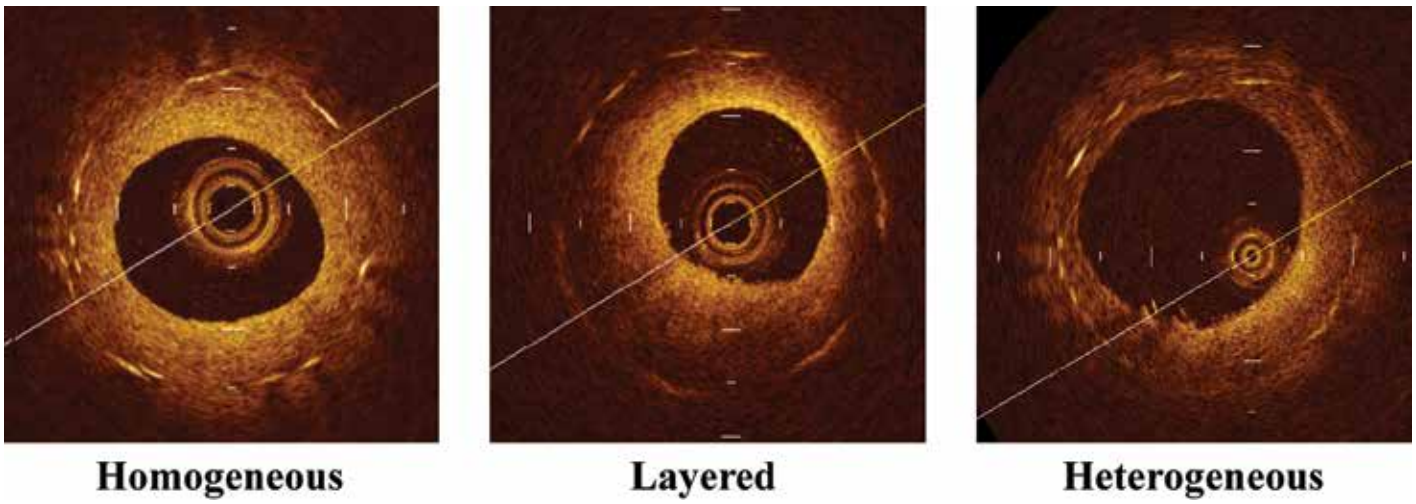

Figure 1. Representative optical coherence tomographic images of each tissue morphologic pattern. Homogeneous pattern: a uniformly signal-rich structure. Heterogeneous pattern: several, varied signal strengths. Layered pattern: a signal-poor appearance with a high-signal band adjacent to the luminal surface.

OCT images (balloon injury, 218 cross-sections from 15 treated sites; stent, 170 cross-sections from 13 sites).

Reference vessel diameter at baseline (mean ± 1 SD) was 3.1 ± 0.3 mm for balloon injury and 2.6 ± 0.4 mm for stenting (P = 0.003). All 3 coronary arteries were overstretched by using conventional semicompliant angioplasty balloons (diameter, 4.0 ± 0.4 mm; length, 15.9 ± 2.7 mm) at average pressure of 13.8 ± 3.4 atm in the proximal part of the vessel and stented distally with a BMS (diameter, 3.0 ± 0.2 mm; length, 12.3 ± 2.8 mm) at average pressure of 10.7 ± 1.7 atm. The B:A ratio achieved was 1.44 ± 0.18 (range, 1.16 to 1.78) for balloon injury and 1.26 ± 0.10 (range, 1.11 to 1.43) for stenting. Baseline lesion and procedural characteristics are summarized in Table 1.

The variables measured at follow-up are shown in Table 2. The injuries led to a late loss of 0.97 ± 0.56 mm in the balloon injury site and 1.11 ± 0.67 mm in the stented site (P = 0.57). The lumen area stenosis and plaque burden at the MLA site were greater in the stented sites than the balloon injury sites (21.7% ± 8.9% compared with 32.8% ± 12.1%, P = 0.01; 30.1% ± 10.1% compared with 44.7% ± 10.1%, P < 0.01, respectively), although stenosis diameter did not differ between the balloon injury and stent groups (19.0% ± 7.9% compared with 22.1% ± 9.4%, P = 0.33). The degree of negative remodeling was significantly larger in the balloon injury group than the stent group (remodeling index, 0.86 ± 0.11 compared with 1.00 ± 0.04, P < 0.01).

Relationship between B/A ratio and stenosis. Relationships between the B:A ratio and the variables measured by QCA and IVUS are shown in Figure 2. Linear regression analysis showed that larger B:A ratios yielded greater late loss and lumen area stenosis at both the balloon injury sites (late loss: r = 0.70, P < 0.01; lumen area stenosis: r = 0.65, P < 0.01) and the stented sites (late loss: r = 0.64, P = 0.02; lumen area stenosis: r = 0.69, P < 0.01). The stent group demonstrated that higher B:A ratios resulted in larger plaque burden (r = 0.72, P < 0.01), but the B/A ratio was not a significant predictor of plaque burden in the balloon injury group. At the balloon injury sites, a higher B:A ratio was significantly associated with greater negative remodeling (r = 0.53, P = 0.04).

Morphologic characterization of neointimal tissue by OCT. In the tissue characterization analysis (Figure 3), the distribution of the optical patterns differed significantly (P < 0.01) between balloon injury sites and stented sites. At the balloon injury site, the predominant pattern was the homogeneous pattern (balloon, 81.7%; stent, 42.4%), whereas almost half of the neointimal tissue in stented sites had a layered pattern (balloon, 13.7%; stent, 49.4%). The heterogeneous pattern occurred infrequently in both balloon injury and stented sites (balloon, 4.6%; stent, 8.2%).

Discussion

In this study, we used IVUS and tissue characterizations by OCT to assess the extent of neointimal hyperplasia in the nonatherosclerotic porcine coronary artery model after balloon overstretch or oversized BMS deployment at a range of B:A ratios. We found that: 1) stent overexpansion produced greater neointimal responses than balloon overstretch injury; 2) higher B;A ratios yielded greater late loss and lumen area stenosis in both balloon injury and stent overexpansion sites; 3) larger B:A ratios resulted in larger plaque burden in stented sites but not balloon injury sites; 4) in balloon injury sites, increased B:A ratios resulted in greater negative remodeling; and 5) OCT revealed differences in neointimal tissue characteristics between balloon overstretch and stent overexpansion sites, in which a layered tissue pattern occurred more frequently in stented sites, whereas most of the neointimal tissue in balloon injury sites had a homogeneous pattern.

Our results show a greater neointimal hyperplastic response to stent overexpansion compared with balloon overstretch injury. This response is apparent as the significant differences in lumen area stenosis and plaque burden at MLA sites. Balloon overstretch injury is caused by the temporary stress on vessel wall during balloon inflation, resulting in a medial injury that leads to the restenotic response. The overstretch dilation caused by the balloon usually creates only a single laceration of the media, which gives rise to an eccentric lesion that rarely protrudes into the lumen. Once the balloon is deflated, the mechanical stretching and tears associated with balloon inflation is followed by elastic recoil of the vessel.[10,18] Our results show a strong relationship between the B:A ratio and the degree of lumen loss: a larger B:A was as-

Table 1. Baseline lesion and procedural characteristics

	Balloon injury (n = 15)	Stent overexpansion (n = 15)	*P*
Reference vessel diameter (mm)	3.1 ± 0.3	2.6 ± 0.4	0.003
Balloon or stent diameter (mm)	4.0 ± 0.4	3.0 ± 0.2	<0.001
Balloon or stent length (mm)	15.9 ± 2.7	12.3 ± 2.8	<0.001
Balloon or stent deployment pressure (atm)	13.8 ± 3.4	10.7 ± 1.7	0.01
Balloon-to-artery ratio	1.44 ± 0.18	1.26 ± 0.10	0.002
Acute gain (mm)	0.7 ± 0.4	0.6 ± 0.4	0.33

Data are presented as mean ± 1 SD.

Table 2. QCA and IVUS measurements at follow-up

	Balloon injury	Stent overexpansion	*P*
QCA	*n* = 14	*n* = 14	
Late loss in vessel diameter (mm)	0.97 ± 0.58	1.05 ± 0.68	0.76
Diameter stenosis (%)	19.0 ± 7.9	22.1 ± 9.4	0.33
IVUS	*n* = 15	*n* = 13	
Lumen area stenosis (%)	21.7 ± 8.9	32.8 ± 12.1	0.01
Plaque burden at MLA site (%)	30.1 ± 10.1	44.7 ± 10.1	0.001
Remodeling index	0.86 ± 0.11	1.00 ± 0.04	0.002

QCA, quantitative coronary analysis; IVUS, intravascular ultrasonography; MLA, minimal lumen area
Data are presented as mean ± 1 SD.

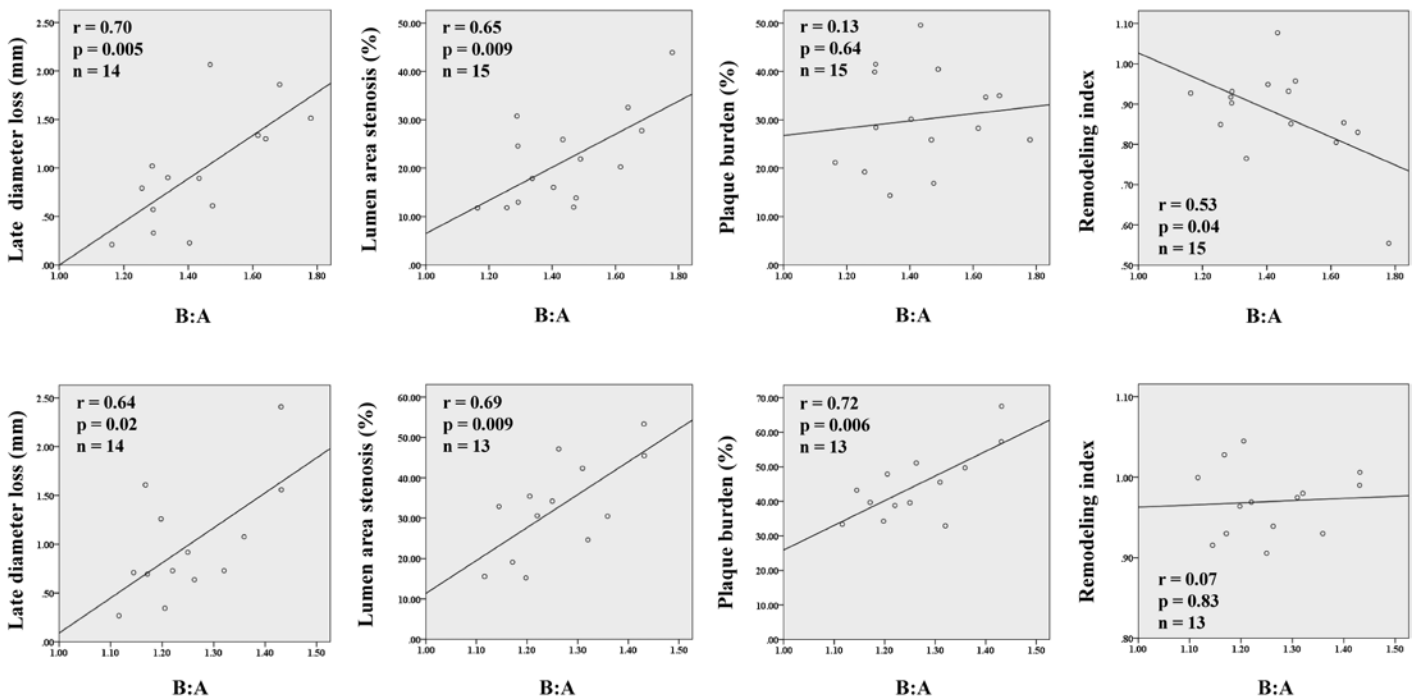

Figure 2. Correlations between balloon-to-artery (B:A) ratios and quantitative parameters assessed by quantitative coronary angiography and intravascular ultrasonography. Upper panels, balloon overstretch injury model; lower panels, stent overexpansion model.

sociated with a stronger negative remodeling after balloon injury. Therefore, in the balloon overstretch model, constrictive negative remodeling rather than neointimal formation may predominantly contribute to luminal narrowing.

Stents, in contrast, can prevent the constrictive remodeling seen after balloon angioplasty, and oversized stents seem to induce multiple injuries instead of a single intimal tear.[7] After the deployment of oversized stents, the injured artery is exposed to

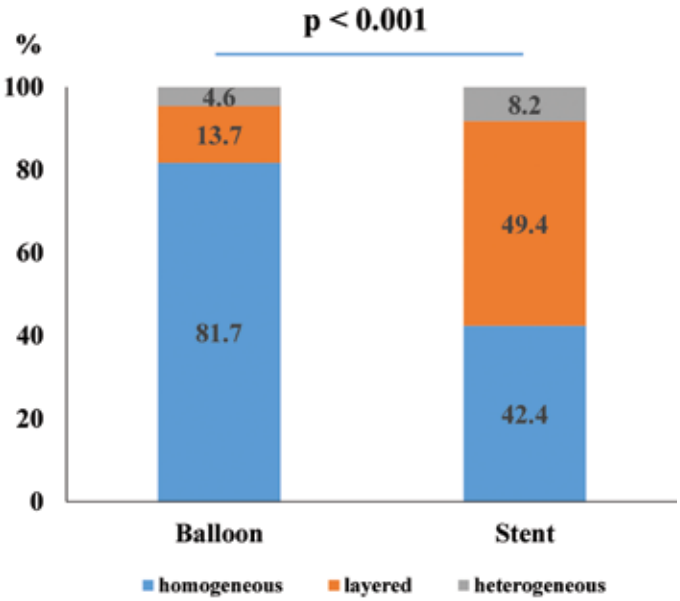

Figure 3. Difference in optical patterns between the balloon overstretch injury model and stent overexpansion model.

prolonged stress, which causes inflammatory reactions. These reactions play an important role in neointimal formation after stenting.[3,7,9,17] Previous studies demonstrated strong correlations between the degree of arterial injury and the extent of the inflammatory reaction as well as between the extent of inflammatory reaction and the degree of neointimal hyperplasia.[3,9,15] Therefore, larger stents can induce greater inflammation, consequently leading to pronounced neointimal proliferation.[3,7,9,15]

In the present study, we classified neointimal and restenotic tissue as having homogeneous, layered, or heterogeneous signal patterns according to the OCT morphology of the lesion.[1] In terms of optical properties, previous studies demonstrated that neointima, which is rich in smooth muscle cells, has a high optical intensity, and restenotic tissue, which rich in proteoglycans, cell matrix, and fibrinoids with a low density of smooth muscle cells, has a low intensity. This difference in signal intensity is due to the different optical wave backscatter patterns. Tissues with a high density of smooth muscle cells are rich in dense collagen fibers, which cause optical wave backscattering.[12,24] A previous pig model applying this OCT pattern classification system to stent restenosis found that highly fibrotic areas showed the homogeneous pattern; that the layered pattern was associated with thick neointima, peri-strut inflammation, and external elastic lamia rupture; and that fibrin deposits were characteristic of the heterogeneous pattern.[8] From these findings, the homogeneous pattern may represent more stable healing process after vessel injury. In our study, very little tissue showed the heterogeneous pattern, which frequently occurs after DES implantation.[8]

Previous studies reported that a homogenous pattern represents a more favorable pattern, indicating more normal healing after BMS implantation.[8,13] However, BMS implantation in our current study predominantly led to layered patterns at the site of injury. A possible explanation for this difference might be the higher B:A ratios at which we deployed BMS compared with the ratios used in other studies. Deep injury might cause pronounced peri-strut inflammation, which might be expressed as a layered pattern on OCT.

Some limitations of this study should be noted. First, the data used for this study were subanalyses from a different, larger study that had both treatment and control groups for assessing restenosis. The original study was not designed to compare differences between balloon injury and stent overexpansion.[1] Therefore, the reference vessel size differed significantly between the balloon injury and the stented sites, potentially distorting the results given that vessel caliber itself is an independent predictor of restenosis.[25] Second, this study was a retrospective analysis of a limited number of cases and was not randomized according to B:A ratio. Third, a key disadvantage of OCT assessment is the limited tissue penetration depth of approximately 1 to 3 mm, which prevents detailed imaging beyond the internal elastic lamina. This characteristic precludes visualization and measurement of the entire plaque and vessel wall. Therefore, parameters such as plaque area and remodeling index cannot be measured and may remain the domain of IVUS, especially after balloon dilatation without stenting.[14]

In conclusion, we found that both balloon overstretch and stent overexpansion consistently produced restenosis in our porcine model. The degree of neointimal proliferation was significantly greater after oversized stents compared with balloon overstretching. Therefore therapies targeted at restenosis might better be studied by using a stent overexpansion restenosis nonatherosclerotic porcine model, given that the greater volumes of neointimal hyperplasia in this model enable more sensitive evaluation of the treatment.

Acknowledgments

This study was indirectly funded by Hamburg University. Yoshiaki Mitsutake received grant support from the International Research Fund for Subsidy of Kyushu University School of Medicine Alumni.

References

1. **Deuse T, Hua X, Wang D, Maegdefessel L, Heeren J, Scheja L, Bolaños JP, Rakovic A, Spin JM, Stubbendorff M, Ikeno F, Länger F, Zeller T, Schulte-Uentrop L, Stoehr A, Itagaki R, Haddad F, Eschenhagen T, Blankenberg S, Kiefmann R, Reichenspurner H, Velden J, Klein C, Yeung A, Robbins RC, Tsao PS, Schrepfer S.** 2014. Dichloroacetate prevents restenosis in preclinical animal models of vessel injury. Nature **509:**641–644.
2. **Gonzalo N, Serruys PW, Okamura T, Van Beusekom HM, Garcia-Garcia HM, Van Soest G, van der Giessen W, Regar E.** 2009. Optical coherence tomography patterns of stent restenosis. Am Heart J **158:**284–293.
3. **Gunn J, Arnold N, Chan KH, Shepherd L, Cumberland DC, Crossman DC.** 2002. Coronary artery stretch versus deep injury in the development of in-stent neointima. Heart **88:**401–405.
4. **Ialenti A, Grassia G, Gordon P, Maddaluno M, Di Lauro MV, Baker AH, Guglielmotti A, Colombo A, Biondi G, Kennedy S, Maffia P.** 2011. Inhibition of in-stent stenosis by oral administration of bindarit in porcine coronary arteries. Arterioscler Thromb Vasc Biol **31:**2448–2454.
5. **Ikeno F, Buchbinder M, Yeung AC.** 2007. Novel stent and delivery systems for the treatment of bifurcation lesions: porcine coronary artery model. Cardiovasc Revasc Med **8:**38–42.
6. **Ikeno F, Inagaki K, Rezaee M, Mochly-Rosen D.** 2007. Impaired perfusion after myocardial infarction is due to reperfusion-induced δPKC-mediated myocardial damage. Cardiovasc Res **73:**699–709.
7. **Karas SP, Gravanis MB, Santoian EC, Robinson KA, Anderberg KA, King SB 3rd.** 1992. Coronary intimal proliferation after balloon injury and stenting in swine: an animal model of restenosis. J Am Coll Cardiol **20:**467–474.

8. **Kim JS, Afari ME, Ha J, Tellez A, Milewski K, Conditt G, Cheng Y, Hua Yi G, Kaluza GL, Granada JF.** 2013. Neointimal patterns obtained by optical coherence tomography correlate with specific histological components and neointimal proliferation in a swine model of restenosis. Eur Heart J Cardiovasc Imaging **15:**292–298.
9. **Kornowski R, Hong MK, Tio FO, Bramwell O, Wu H, Leon MB.** 1998. In-stent restenosis: contributions of inflammatory responses and arterial injury to neointimal hyperplasia. J Am Coll Cardiol **31:**224–230.
10. **Mintz GS, Popma JJ, Pichard AD, Kent KM, Satler LF, Wong C, Hong MK, Kovach JA, Leon MB.** 1996. Arterial remodeling after coronary angioplasty: a serial intravascular ultrasound study. Circulation **94:**35–43.
11. **Mintz GS, Nissen SE, Anderson WD, Bailey SR, Erbel R, Fitzgerald PJ, Pinto FJ, Rosenfield K, Siegel RJ, Tuzcu EM, Yock PG.** 2001. American College of Cardiology Clinical Expert Consensus document on standards for acquisition, measurement and reporting of intravascular ultrasound studies (IVUS). A report of the American College of Cardiology Task Force on clinical expert consensus documents. J Am Coll Cardiol **37:**1478–1492.
12. **Nagai H, Ishibashi-Ueda H, Fujii K.** 2010. Histology of highly echolucent regions in optical coherence tomography images from 2 patients with sirolimus-eluting stent restenosis. Catheter Cardiovasc Interv **75:**961–963.
13. **Nagoshi R, Shinke T, Otake H, Shite J, Matsumoto D, Kawamori H, Nakagawa M, Kozuki A, Hariki H, Inoue T, Ohsue T, Taniguchi Y, Iwasaki M, Nishio R, Hiranuma N, Konishi A, Kinutani H, Miyoshi N, Takaya T, Yamada S, Yasaka Y, Hayashi T, Yokoyama M, Kato H, Kadotani M, Ohnishi Y, Hirata K.** 2013. Qualitative and quantitative assessment of stent restenosis by optical coherence tomography: comparison between drug-eluting and bare-metal stents. Circ J **77:**652–660.
14. **Raffel OC, Akasaka T, Jang IK.** 2008. Cardiac optical coherence tomography. Heart **94:**1200–1210.
15. **Russo RJ, Silva PD, Yeager M.** 2007. Coronary artery overexpansion increases neointimal hyperplasia after stent placement in a porcine model. Heart **93:**1609–1615.
16. **Schwartz RS, Murphy JG, Edwards WD, Camrud AR, Vliestra RE, Holmes DR.** 1990. Restenosis after balloon angioplasty: a practical proliferative model in porcine coronary arteries. Circulation **82:**2190–2200.
17. **Schwartz RS, Huber KC, Murphy JG, Edwards WD, Camrud AR, Vliestra RE, Holmes DR.** 1992. Restenosis and the proportional neointimal response to coronary artery injury: results in a porcine model. J Am Coll Cardiol **19:**267–274.
18. **Serruys PW, Luijten HE, Beatt KJ, Geuskens R, de Feyter PJ, van den Brand M, Reiber JH, ten Katen HJ, van Es GA, Hugenholtz PG.** 1988. Incidence of restenosis after successful coronary angioplasty: a time-related phenomenon. A quantitative angiographic study in 342 consecutive patients at 1, 2, 3, and 4 months. Circulation **77:**361–371.
19. **Suzuki Y, Lyons JK, Yeung AC, Ikeno F.** 2007. In vivo porcine model of reperfused myocardial infarction: in situ double staining to measure precise infarct area/area at risk. Catheter Cardiovasc Interv **71:**100–107.
20. **Suzuki Y, Lyons JK, Yeung AC, Ikeno F.** 2008. The porcine restenosis model using thermal balloon injury: comparison with the model by coronary stenting. J Invasive Cardiol **20:**142–146.
21. **Suzuki Y, Yeung AC, Ikeno F.** 2009. The preclinical animal model in the translational research of interventional cardiology. JACC Cardiovasc Interv **2:**373–383.
22. **Suzuki Y, Yeung AC, Ikeno F.** 2011. The representative porcine model for human cardiovascular disease. J Biomed Biotechnol **2011:**1–10.
23. **Tada T, Kadota K, Hosogi S, Miyake K, Ohya M, Amano H, Izawa Y, Kanazawa T, Kubo S, Ichinohe T, Hyoudou Y, Hayakawa Y, Sabbah MM, Otsuru S, Hasegawa D, Habara S, Tanaka H, Fuku Y, Katoh H, Goto T, Mitsudo K.** 2015. Association between tissue characteristics assessed with optical coherence tomography and midterm results after percutaneous coronary intervention for in-stent restenosis lesions: a comparison between balloon angioplasty, paclitaxel-coated balloon dilatation, and drug-eluting stent implantation. Eur Heart J Cardiovasc Imaging **16:**1101–1111.
24. **Teramoto T, Ikeno F, Otake H, Lyons JK, van Beusekom HM, Fearon WF, Yeung AC.** 2010. Intriguing peri-strut low-intensity area detected by optical coherence tomography after coronary stent deployment. Circ J **74:**1257–1259.
25. **West NE, Ruygrok PN, Disco CM, Webster MW, Lindeboom WK, O'Neill WW, Mercado NF, Serruys PW.** 2004. Clinical and angiographic predictors of restenosis after stent deployment in diabetic patients. Circulation **109:**867–873.